


# Concomitant administration of radiation with eribulin improves the survival of mice harboring intracerebral glioblastoma

Shunichiro Miki<sup>1,2,3</sup> | Shoji Imamichi<sup>4</sup> | Hiroaki Fujimori<sup>4</sup> | Arata Tomiyama<sup>2,5</sup> | Kenji Fujimoto<sup>2,6</sup> | Kaishi Satomi<sup>2,7</sup> | Yuko Matsushita<sup>1,2</sup> | Sanae Matsuzaki<sup>1,2</sup> | Masamichi Takahashi<sup>1,2</sup> | Eiichi Ishikawa<sup>3</sup> | Tetsuya Yamamoto<sup>3,8</sup> | Akira Matsumura<sup>3</sup> | Akitake Mukasa<sup>6,9</sup> | Ryo Nishikawa<sup>10</sup> | Kenkichi Masutomi<sup>11</sup> | Yoshitaka Narita<sup>1</sup> | Mitsuko Masutani<sup>4,12</sup> | Koichi Ichimura<sup>2</sup> 

<sup>1</sup>Department of Neurosurgery and Neuro-Oncology, National Cancer Center Hospital, Tokyo, Japan

<sup>2</sup>Division of Brain Tumor Translational Research, National Cancer Center Research Institute, Tokyo, Japan

<sup>3</sup>Department of Neurosurgery, Faculty of Medicine, University of Tsukuba, Ibaraki, Japan

<sup>4</sup>Division of Chemotherapy and Clinical Research, National Cancer Center Research Institute, Tokyo, Japan

<sup>5</sup>Department of Neurosurgery, National Defense Medical College, Tokorozawa, Japan

<sup>6</sup>Department of Neurosurgery Graduate School of Medical Sciences, Kumamoto University, Kumamoto, Japan

<sup>7</sup>Department of Pathology and Clinical Laboratories, National Cancer Center Hospital, Tokyo, Japan

<sup>8</sup>Department of Neurosurgery, Graduate School of Medicine, Yokohama City University, Yokohama, Japan

<sup>9</sup>Department of Neurosurgery, the University of Tokyo, Tokyo, Japan

<sup>10</sup>Department of Neuro-Oncology/Neurosurgery, Saitama Medical University International Medical Center, Hidaka, Japan

<sup>11</sup>Division of Cancer Stem Cell, National Cancer Center Research Institute, Tokyo, Japan

<sup>12</sup>Department of Frontier Life Sciences, Nagasaki University Graduate School of Medicine, Nagasaki, Japan

## Correspondence

Koichi Ichimura, Division of Brain Tumor Translational Research, National Cancer Center Research Institute, Tokyo, Japan.  
Email: kichimur@ncc.go.jp

## Funding information

Practical Research for Innovative Cancer Control program of Japan Agency for Medical Research and Development grant no: 17ck0106140 h0003

Glioblastoma is the most common and devastating type of malignant brain tumor. We recently found that eribulin suppresses glioma growth in vitro and in vivo and that eribulin is efficiently transferred into mouse brain tumors at a high concentration. Eribulin is a non-taxane microtubule inhibitor approved for breast cancer and liposarcoma. Cells arrested in M-phase by chemotherapeutic agents such as microtubule inhibitors are highly sensitive to radiation-induced DNA damage. Several recent case reports have demonstrated the clinical benefits of eribulin combined with radiation therapy for metastatic brain tumors. In this study, we investigated the efficacy of a combined eribulin and radiation treatment on human glioblastoma cells. The glioblastoma cell lines U87MG, U251MG and U118MG, and SJ28 cells, a patient-derived sphere culture cell line, were used to determine the radiosensitizing effect of eribulin using western blotting, flow cytometry and clonogenic assay. Subcutaneous and intracerebral glioma xenografts were generated in mice to assess the efficacy of the combined treatment. The combination of eribulin and radiation

This is an open access article under the terms of the Creative Commons Attribution-NonCommercial License, which permits use, distribution and reproduction in any medium, provided the original work is properly cited and is not used for commercial purposes.

© 2018 The Authors. *Cancer Science* published by John Wiley & Sons Australia, Ltd on behalf of Japanese Cancer Association.

enhanced DNA damage in vitro. The clonogenic assay of U87MG demonstrated the radiosensitizing effect of eribulin. The concomitant eribulin and radiation treatment significantly prolonged the survival of mice harboring intracerebral glioma xenografts compared with eribulin or radiation alone ( $P < .0001$ ). In addition, maintenance administration of eribulin after the concomitant treatment further controlled brain tumor growth. Aberrant microvasculature was decreased in these tumors. Concomitant treatment with eribulin and radiation followed by maintenance administration of eribulin may serve as a novel therapeutic strategy for glioblastomas.

**KEYWORDS**

angiogenesis, eribulin, microenvironment, radiation, radiosensitization

## 1 | INTRODUCTION

Glioblastoma (GBM) is the most common malignant brain tumor and one of the most devastating cancers in humans. Even with intensive chemoradiotherapy after surgical resection, patients' median overall survival (OS) is  $<2$  years.<sup>1</sup> A series of large-scale genomic studies in the last decade have provided a vast amount of information regarding the genetic alterations in GBM, which may lead to a better understanding of these tumors.<sup>2-4</sup> It has, however, also been revealed that the extensive molecular heterogeneity in GBM may be responsible for the failure of a number of molecular targeting therapies.<sup>5-7</sup> A novel therapeutic strategy for GBM is desperately needed.

For a newly diagnosed GBM, a maximum safe surgical resection followed by combined radiation therapy and chemotherapy with temozolomide (TMZ) is the current standard of care. Radiation suppresses the growth of GBM and prolongs the survival of patients with GBM, and, therefore, it is central to the treatment of GBM.<sup>8</sup> Radiosensitization by arresting the cell cycle in M-phase has been shown to increase the efficacy of radiation. A number of previous reports have shown that cells arrested in M-phase by chemotherapy are highly sensitive to DNA damage and that cell death is efficiently induced in some cases, a phenomenon described as mitotic catastrophe.<sup>9-13</sup>

Eribulin methylate (eribulin), a non-taxane inhibitor of microtubule dynamics, has been approved for late-stage and refractory breast cancer, liposarcoma and sarcoma in many countries. The mode of action is reported to be microtubule inhibition-dependent apoptosis and normalization of the tumor microenvironment through vascular remodeling.<sup>14-20</sup> The distribution of eribulin to the normal brain in mice has been reported to be low, and the clinical benefit of this agent for GBM is considered to be limited.<sup>21,22</sup> However, recently, we found that eribulin penetrates brain tumor tissues at a high concentration in an intracerebral mouse brain tumor model and suppresses tumor growth, suggesting that eribulin may have activity against GBM in a clinical setting (Takahashi, manuscript submitted). In fact, consistent with its anti-microtubule activity, eribulin treatment with radiation therapy has been shown to be effective against brain metastasis from breast cancer in several case reports.<sup>23-26</sup>

Because radiation is a part of the standard therapy for newly diagnosed GBM, studying the effect of eribulin as a radiosensitizer has great clinical value.

In this study, we investigated the effect and mechanism of a combined eribulin and radiation treatment on suppressing glioma growth in an intracerebral GBM xenograft model. We showed that the combination induced DNA damage in vitro and prolonged survival in an intracranial xenograft mouse model. In addition, the continued administration of eribulin after radiation prevented tumor recurrence and reduced abnormal angiogenesis. Our results suggest that the concomitant administration of eribulin with radiation may serve as an effective novel treatment strategy for GBM.

## 2 | MATERIALS AND METHODS

### 2.1 | Compound and cell lines

Eribulin (Halaven) was purchased from Eisai (Tsukuba, Japan). The eribulin dose per administration for intracranial tumors was 0.5 mg/kg, which is equivalent to the clinical dose in humans. For subcutaneous tumors, 0.05 or 0.5 mg/kg was used (see below). Injecting these doses 3 times per week for a long period of time was found to be safe and tolerable in a preliminary experiment even with whole brain radiation therapy (data not shown). The human glioma cell lines U87MG, U118MG and U251MG were provided by Professor Collins, University of Cambridge, UK. All cell lines have been genotyped (Takahashi, manuscript submitted). SJ28 cells, a stem-like glioma cell line, were directly established from a surgical specimen of a glioblastoma patient at the National Cancer Center Hospital<sup>27</sup> and serially passaged under non-adherent culture conditions at 37°C/5% CO<sub>2</sub> in serum-free F12/DMEM supplemented with epidermal growth factor and fibroblast growth factors.<sup>28</sup>

### 2.2 | Western blotting

Preparation of cell lysates, immunoblotting and immunoprecipitation were performed as described previously.<sup>29</sup> Membranes were immunoblotted with antibodies against phospho-histone H3 (Cell

Signaling; #9701, 1:2000), phospho-histone H2A.X ( $\gamma$ H2AX, Millipore; #05-636, 1:2000), caspase-3 (Cell Signaling; #9662, 1:1000), Cleaved PARP (Asp214) (D64E10) XP (Cell Signaling; #5625, 1:2000), GAPDH (Cell Signaling; #2118S, 1:3000) or  $\beta$ -actin (Sigma; A1978, 1:10 000). Signals were detected using a HRP-conjugated secondary antibody (Cell Signaling; #7074S and #7076S, 1:3000) and documented using an Amersham Imager 600 (GE Healthcare).

### 2.3 | Clonogenic assay

The clonogenic assay was performed as previously described with some modifications.<sup>30</sup> Briefly, cell lines were seeded in 25-cm<sup>2</sup> flasks with 5 mL of culture medium 20 hours before irradiation. Then, an equal amount of eribulin or control solution was added to the culture flask 8 hours before irradiation. Cells were irradiated at 2, 4 or 6 Gy. Following irradiation, the cells were incubated at 37°C with 5% CO<sub>2</sub>. After 10-12 days, surviving colonies were fixed with 4% buffered formalin solution (Muto Pure Chemical) and stained with 0.02% crystal violet solution (Sigma, C6158-50G). Colonies composed of approximately 50 cells or more were counted. Cell survival was calculated by dividing the number of cell colonies by the number of inoculated cells and plating efficiencies of the control cells in each condition. The results were then calculated from the average of 3 independent experiments.

### 2.4 | Immunohistochemistry

Resected mouse brains were sliced and fixed in 10% buffered formalin solution for 1 day and then embedded in paraffin. The presence of a tumor was determined by H&E staining. For mean vascular area (MVA) analysis, sections were incubated with goat anti-rat CD34 polyclonal antibody (R&D Systems; #AF4117, 1:100) and then with the secondary antibody (anti-goat IgG- peroxidase; Sigma-Aldrich, A5420, 1:200) and detected with the 3,3'-diaminobenzidine substrate (Sigma-Aldrich). Slides were counter-stained with hematoxylin. Quantification of the CD34-positive vascular area was performed using ImageJ software.<sup>31</sup> MVA was calculated as the average of 5 vascular hot spots (500 × 500  $\mu$ m<sup>2</sup> in each spot) chosen in each sample.

### 2.5 | Flow cytometry

Flow cytometry analysis was performed as previously described.<sup>30</sup> Briefly, after eribulin (0.1, 1 and 10 nmol/L) exposure (12 and 24 hours), cells were harvested and fixed with 70% ethanol, treated with RNase A, stained with propidium iodide (PI), and analyzed on a FACSCalibur flow cytometer (Beckton Dickinson, Mountain View, CA, USA).

### 2.6 | Quantification of cell death rate

The rate of cell death induction was assayed by co-staining of treated cells with propidium iodide (PI, Thermo Fisher Scientific) and

DAPI (Thermo Fisher Scientific). Fluorescence images of PI and DAPI were acquired using an Olympus CKX53 microscope, and the numbers of PI-positive cells and DAPI-positive cells in each image were obtained using ImageJ software (NIH). The rate of cell death was calculated as (number of PI-positive cells)/(number of DAPI-positive cells) × 100 (%).

### 2.7 | Animals and tumor models

Glioma cell xenografts were generated as described previously.<sup>32</sup> Briefly, U87MG cells ( $1 \times 10^5$  cells) for BALB/c-*nu/nu* female mice (Charles River Laboratories Japan) or SJ28 cells ( $2.5 \times 10^5$  cells) for SCID-Beige female mice (Charles River Laboratories Japan) were inoculated into the right cerebral hemisphere with a Hamilton syringe and stereotactic micro-injector (Narishige, Tokyo, Japan) in 2  $\mu$ L of PBS. The injection site coordinates were 1-mm anterior and 2-mm lateral to the bregma and 3-mm deep from the dura mater. For the subcutaneous model, U87MG cells ( $2 \times 10^6$  cells in 100  $\mu$ L PBS) were injected subcutaneously into the left leg of BALB/c-*nu/nu* male mice (Charles River Laboratories Japan). The mice were subjected to irradiation (2-4 Gy) restricted to the left leg or head while the rest of the body was protected by a lead shield. All treatments were performed when the mice were 5-7 weeks old. Eribulin or saline was intraperitoneally injected. The mouse weights and tumor sizes were measured at least twice a week before starting treatment, and tumor volume was calculated using the long axis and minor axis as described previously.<sup>33</sup> All mice were irradiated under anesthesia. All animal studies were approved by the Animal Experimental Committee of the National Cancer Center and were performed in accordance with the Guidelines for Animal Experiments of the National Cancer Center, which concur with the ethical guidelines for experimental animals in Japan.

### 2.8 | Irradiation

Cells were exposed to  $\gamma$ -irradiation using a Gamma-Cell Exactor 40 (with 137-Cs) at approximately 1 Gy/min at the National Cancer Center Research Institute in Japan. Mice were irradiated by X-rays using a CP-160 (Acrobio) at approximately 0.33 Gy/min. Mice were stabilized in irradiation containers during irradiation of the left leg. The radiation dose for the mice was set to 4 Gy each time to simulate the clinical whole brain radiation dose of 2-4 Gy.<sup>34</sup>

### 2.9 | Statistics

Two-way ANOVA was performed for the *in vitro* clonogenic assay, two-way RM ANOVA with Bonferroni post-tests were performed for *in vivo* subcutaneous tumor data, and ANOVA with Bonferroni post-tests were performed for the MVA analysis and abnormal mitotic cell count analysis for statistical comparisons between groups. The Student *t* test was performed for cell death rate. *P*-values below .05 were considered significant. A log-rank test was performed for the Kaplan-Meier survival curve. All analyses were performed using GraphPad Prism 5 software.

### 3 | RESULTS

#### 3.1 | Eribulin arrests the cell cycle of glioma cell lines, induces DNA damage in mitotic phase when combined with radiation, and shows a sensitizing interaction in vitro

We first investigated the effect of eribulin on inhibiting microtubule dynamics in the U87MG glioma cell line using flow cytometry. As previously reported,<sup>18</sup> we confirmed that eribulin induced cell cycle arrest in G2/M-phase (Figure 1A). The phosphorylated form of histone H3 was increased upon exposure to eribulin in a dose-dependent manner with or without radiation (Figure 1B), suggesting that M-phase arrest was induced by eribulin. Second, the efficacy of the combination of irradiation and eribulin was assessed by examining the cell-cycle status and DNA damage in irradiated and/or eribulin-treated U87MG cells. Upregulation of phosphorylated H2AX ( $\gamma$ H2AX) was evident 60 minutes after radiation was administered concomitantly with 1 or 10 nmol/L eribulin (Figure 1B). Taken together, these data suggested that DNA damage may be induced by irradiation in U87MG cells arrested at M-phase by eribulin. We then assessed the death rate of U87MG and U251MG cells upon exposure to eribulin and/or irradiation (Figure 1C). Increased cell death was induced by eribulin, and this was significantly ( $P < .05$ ,  $t$  test) enhanced by addition of radiation (8 Gy). To investigate the mechanism of cell death, the caspase-dependent apoptotic pathway was studied, as it is one of the best-characterized mechanisms of programmed cell death. Cleaved caspase-3 levels were increased upon exposure to 10 nmol/L eribulin in all cell lines tested (Figure S1A). However, the enhancement of this by the addition of radiation was not clearly demonstrated. We further studied another apoptosis marker, cleaved PARP, to assess the involvement of the caspase cascade in eribulin/irradiation-induced cell death (Figure S1B). Cleaved PARP levels were significantly increased when 0.5 nmol/L eribulin was combined with irradiation compared with irradiation or eribulin alone in U251MG cells. However, the synergistic or additive effects of eribulin/irradiation on caspase-dependent apoptosis were not clear at other doses of eribulin in U251MG or at any doses in U87MG cells (Figure S1B). We further evaluated the involvement of the caspase pathway in eribulin/irradiation-induced cell death (revised Figure 1C) by inhibiting caspase (Figure S1C). Death rates of neither U87MG nor U251MG cells treated with a combination of eribulin (5 nmol/L) and irradiation were reduced by addition of pan-caspase inhibitor z-VAD-FMK (VAD), while cisplatin (CDDP)-induced caspase-dependent cell death was significantly reduced ( $P < .01$ ,  $t$  test). Thus, the increased cell death caused by addition of radiation to eribulin appeared to include a caspase-independent mechanism. To further validate the radiosensitizing effect of eribulin, we performed a clonogenic assay using U87MG cells. The adjusted killing curve revealed a radio-sensitizing effect of eribulin (Figure S1D). Taken together, these results suggested that the combination of eribulin and radiation may be effective against GBM.

#### 3.2 | Combined effects of eribulin and radiation in vivo

The radiosensitizing effect of eribulin was then examined in vivo by treating xenografted mice with either eribulin or radiation alone or both in combination. For the intracerebral glioblastoma xenograft model, 0.5 mg/kg eribulin per administration, which is equivalent to the clinical dose for humans, was intraperitoneally administered 6 times in 12 days (Figure 2A). The local radiation dose was set to  $3 \times 4$  Gy, and the body of the mice was protected from radiation. For combined treatment, the xenografted tumors were irradiated 24 hours after eribulin injection, as was done in vitro. The results showed that radiation alone did not have a survival benefit over the untreated control, whereas 0.5 mg/kg eribulin significantly prolonged the survival of mice harboring intracerebral U87MG xenografts (Figure 2B). When radiation and eribulin were concomitantly given, however, radiation significantly prolonged the survival of mice with intracerebral tumors compared to that in mice treated with either radiation or eribulin alone. These data supported the idea that eribulin has a radiosensitizing effect on mouse U87MG brain xenografts.

For the subcutaneous xenograft model, the radiosensitization effect of eribulin was examined at a dose of 0.05 mg/kg given 3 times in 6 days instead of 0.5 mg/kg because 6 days of treatment with 0.5 mg/kg eribulin alone was sufficient to completely suppress the growth of subcutaneous tumors (Figure S2). The results showed that eribulin (0.05 mg/kg) and radiation given concomitantly significantly enhanced the growth suppression of the subcutaneous tumor compared to that induced by either eribulin or radiation alone (Figure S3). To further clarify the growth-suppressive effects of eribulin, radiation, and eribulin and radiation combined, we retrieved tissues from the brains of mice harboring intracerebral xenografts treated with each regimen and compared them morphologically using H&E-stained sections (Figure 2C). In tumors treated with radiation alone, although enlarged multi-nucleated cells and marked neutrophil invasion with phagocytosed dead cells were seen (Figure 2C, upper right, arrow head), there was no difference in tumor volume compared to that in untreated tumors. The histology of tumors treated with eribulin alone revealed significantly ( $P < .05$ ; one-way ANOVA Bonferroni post-test) increased numbers of "abnormal mitotic cells,"<sup>35</sup> suggesting that eribulin may have an inhibitory effect on microtubule dynamics of tumor cells (Figure 2C, lower left, arrow, Figure S4). Tumor tissues treated with the combination of eribulin and radiation exhibited a markedly lower tumor volume and distinct cellular morphology compared to those of tumors treated with radiation or eribulin alone (Figure 2C, lower right). Cellular density was also low, and many flattened and enlarged cells were observed. A similar survival benefit of the combined treatment was also confirmed in SJ28 cells, a patient-derived sphere culture cell line (Figure S5). In this model, the radiation dose was reduced to  $3 \times 2$  Gy because the mouse strain used in this experiment (SCID/Beige) could not tolerate  $3 \times 4$ -Gy radiation (data not shown). These results strongly suggested that the combined therapy of eribulin and irradiation had a synergistic effect in in vivo brain tumor models.

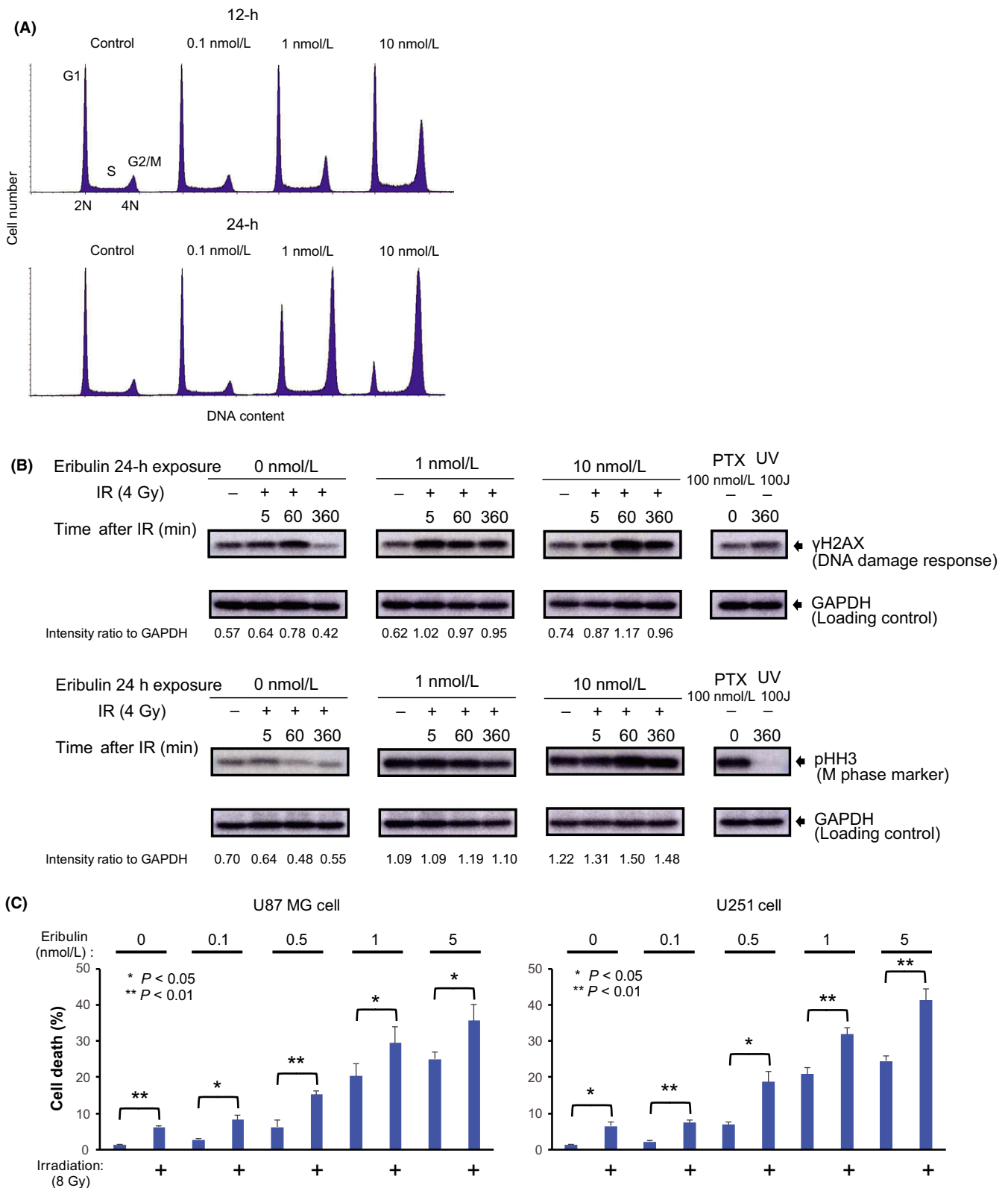


**FIGURE 1** Effects of eribulin and irradiation on human glioma cell lines in vitro. A, The cell cycle status of U87MG cells was analyzed after incubation with various doses of eribulin for 12 and 24 h by flow cytometry with propidium iodide staining. B, U87MG cells were treated with eribulin at 3 different doses 24 h before irradiation and analyzed by western blotting in a time course up to 6 h. PTX; paclitaxel treatment at 100 nmol/L for 24 h. UV; 24 h after ultra-violet ray irradiation at 254 nm. C, The indicated glioblastoma cell lines were seeded on collagen-coated culture dishes. After 16 h, the cells were treated with the indicated dose of eribulin followed by irradiation (8 Gy). The cells were further cultured for 72 h, and induction of cell death was quantified as described in the Materials and Methods section. Data shown are mean values  $\pm$  SD from 3 independent experiments

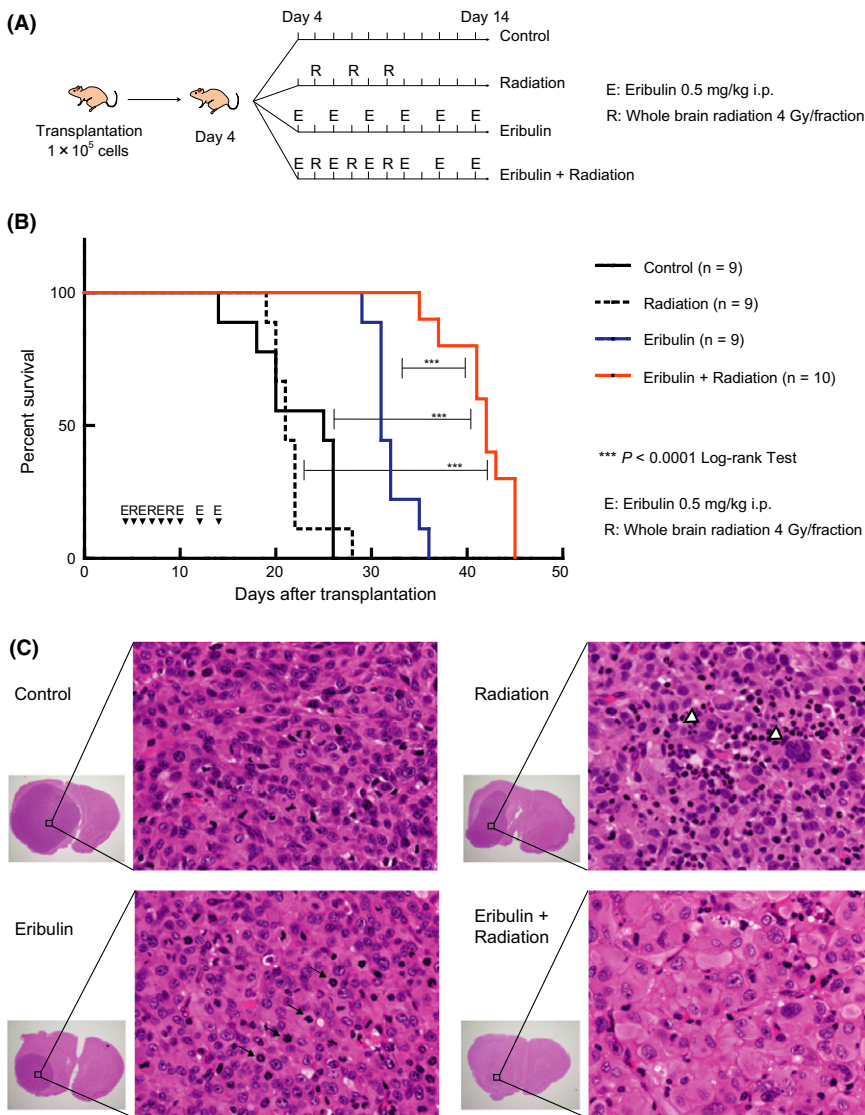


**FIGURE 2** Effects of eribulin and irradiation on intracranial U87MG cell xenograft mouse models. A, Scheme showing the treatment schedules of the 4 regimens: Control, saline injection, and no radiation therapy; Radiation, saline injection, and irradiation (4 Gy  $\times$  3); Eribulin, eribulin (0.5 mg/kg) injection, and no radiation therapy; and Eribulin + Radiation, eribulin (0.5 mg/kg) injection, and irradiation (4 Gy  $\times$  3). B, A Kaplan-Meier survival curve of mice harboring U87MG intracerebral xenografts treated with eribulin and radiation. There were 9-10 mice in each group. C, Representative H&E-stained histological images of U87MG xenografts at the end of the treatment schedule

### 3.3 | Survival benefits of the maintenance administration of eribulin after the combined therapy

We further determined whether the continued administration of eribulin produced a more sustained effect on the inhibition of microtubule dynamics and suppression of tumor growth. To validate this hypothesis, we performed another set of experiments using U87MG brain xenografted mice (Figure 3). In one set of animals ( $n = 6$ ), eribulin (0.5 mg/kg) was given intraperitoneally 3 times/week continually until the mice had deteriorated and were euthanized. In another set ( $n = 7$ ), 4 Gy radiation was given 3 times in the first week alone, and eribulin (0.5 mg/kg, 3 times/week) was given continually until the mice had deteriorated (Figure 4). The survival rates of the mice continually treated with eribulin with or without radiation were compared with those of untreated U87MG brain xenografted mice ( $n = 3$ ) or those treated with radiation alone ( $n = 3$ ). The results showed that while the animals continually treated with eribulin alone survived significantly longer than the untreated controls or those treated with radiation alone, those treated with

radiation and continual eribulin lived significantly longer than those treated with eribulin alone; only 2 mice died as a result of the brain tumor 80 days after the initiation of the treatment (Figure 3B). These results further confirmed the synergistic effect of eribulin and radiation, which suggests that the cytostatic effect of the long-term administration of 0.5 mg/kg eribulin after concomitant therapy with radiation may lead to sustained tumor control.

### 3.4 | Effects of eribulin on tumor vascular area after radiation in intracranial xenograft models

It is widely known that abnormal angiogenesis occurs after tumor irradiation and that it may contribute to tumor recurrence.<sup>36,37</sup> Since the suppressive effect of eribulin on vascular remodeling was recently reported,<sup>19,20</sup> we determined whether eribulin administration neutralized the radiation-induced abnormal vascularization in tumors. The treatment schedule was optimized to evaluate vascular remodeling,<sup>20</sup> especially to assess the late effects of radiation (Figure 4A). Figure 4B presents representative histopathological images.

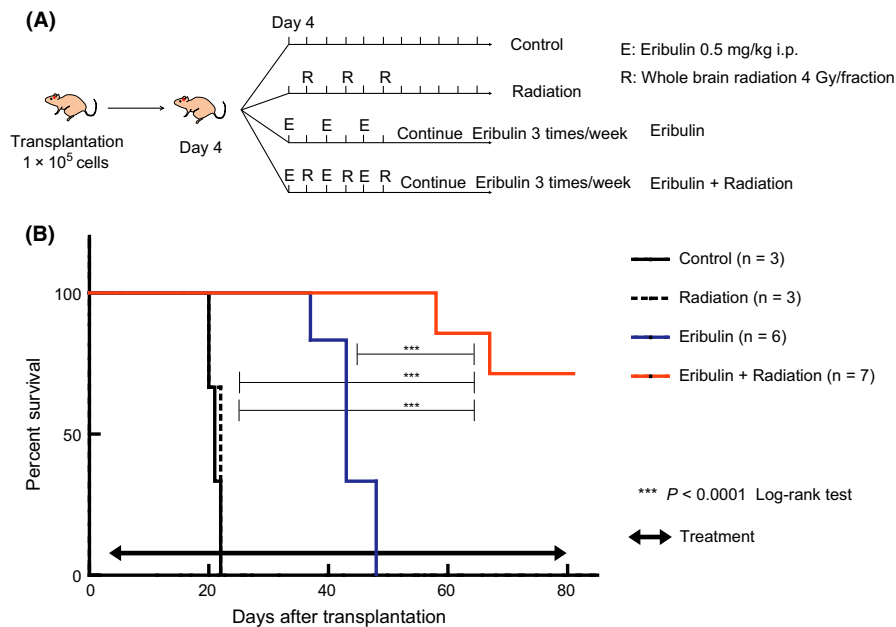


**FIGURE 3** Effects of the maintenance administration of eribulin after concomitant administration of irradiation in intracranial U87MG xenograft mouse models. A, Scheme showing the treatment schedules of the 4 regimens: (i) 3 times/wk continual saline injection and no irradiation; (ii) 3 times/wk continual saline injection and irradiation (4 Gy  $\times$  3); (iii) 3 times/wk continual eribulin (0.5 mg/kg) injection and no irradiation; and (iv) 3 times/wk continual eribulin (0.5 mg/kg) injection and irradiation (4 Gy  $\times$  3). B, A Kaplan-Meier curve of mice harboring U87MG intracranial xenografts treated with the concomitant administration of eribulin and irradiation followed by continual (maintenance) administration of eribulin. There were 3 mice in the control and irradiated groups, 6 mice in the eribulin-treated group and 7 mice in the combination treatment group

Although the difference was not statistically significant, the irradiated xenografts tended to have a higher MVA compared to that of the control group. When eribulin was given concomitantly with or after irradiation, however, MVA was significantly higher in the eribulin +/-after irradiated group compared with that in the radiation alone group (Figure 4C). These results suggested that eribulin may normalize the radiation-induced aberrant vascular microenvironment.

## 4 | DISCUSSION

In the present study, we demonstrated that eribulin exerted a synergistic effect with radiation to suppress the growth of glioma cells (Figure 1). Moreover, the concomitant eribulin and radiation treatment significantly prolonged the survival of mice with intracerebral xenografts of gliomas compared to that of mice treated with eribulin or radiation monotherapy (Figure 2). We previously showed that intravenously administered eribulin reached xenografted mouse brain tumor tissues at a high concentration comparable to that in plasma, and that a clinically equivalent dose of eribulin significantly prolonged survival of mice intracerebrally xenografted with U87MG or several other patient-derived serum-free cultured glioma cells (Takahashi, manuscript submitted). Together with these data, our results strongly suggest that the combined eribulin and radiation treatment may serve as an attractive, novel therapeutic strategy for newly diagnosed GBM. The potential mechanisms by which eribulin and

radiation cooperate to suppress glioma growth are discussed below (Figure 5).

First, we demonstrated that DNA damage was induced by the combined eribulin and radiation treatment. It is plausible that radiation-induced DNA damage was enhanced by cell cycle arrest, most likely at M-phase, by eribulin. We showed that the combination of eribulin and radiation increased cell death in glioma cells through a caspase-independent mechanism. We further validated the radiosensitizing effect of eribulin. The combined eribulin and radiation treatment showed increased DNA damage and death rates in U87MG cells, suggesting the synergistic effect of the combined treatment (Figure S1D). It should be noted that the dosage of eribulin was reduced to 0.05 nmol/L in this assay, which was below the level at which eribulin induced cell cycle arrest, because eribulin itself has a strong colony formation-inhibiting activity in glioma cell lines. We hypothesize that the mechanism for this effect may be at least in part due to inhibition of microtubule dynamics, which may enhance the cytotoxic effect of radiation. In the in vivo experiments, eribulin alone significantly increased the number of "abnormal mitotic cells," suggesting that eribulin may have an inhibitory effect on microtubule dynamics (Figure 2C, Figure S4). The fact that these cells were not seen in the tumor tissues treated with the combination of eribulin and radiation therapy suggests the possibility that they were mostly eradicated by irradiation because of their enhanced radiation sensitivity conferred by eribulin. Although determination of the exact mechanisms of cell death induced by the combination of eribulin and

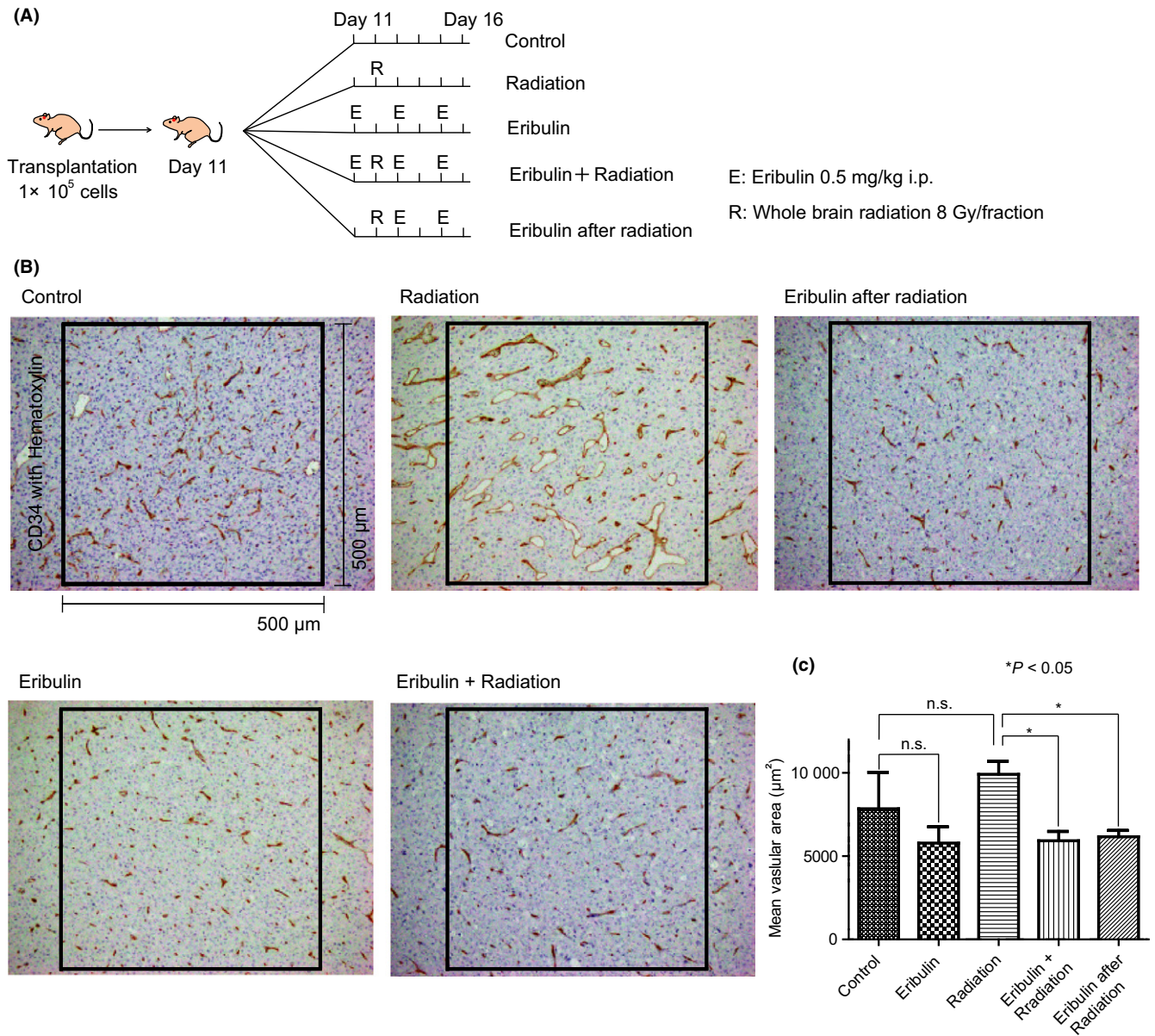


**FIGURE 4** Effects of eribulin on the microvasculature in intracranial U87MG xenograft mouse models. The irradiation dose was increased to 8 Gy to observe its effect on the microvasculature. A, Scheme showing the treatment schedules of the regimen: (i) Saline injection and no irradiation; (ii) saline injection and single fraction of 8 Gy irradiation only; (iii) eribulin (0.5 mg/kg) injection and no irradiation; (iv) eribulin (0.5 mg/kg) injection and a single fraction of 8 Gy irradiation; and (v) eribulin (0.5 mg/kg) injection only after irradiation. The control group contained 4 mice, and the other groups contained 3 mice. All mice were euthanized on day 16. B, Representative histological images of immunohistochemical staining with CD34, an endothelial marker, and counterstaining with hematoxylin are shown. C, A quantitative analysis of the mean vascular area. Data are shown as the mean  $\pm$  SD. n.s., not significant

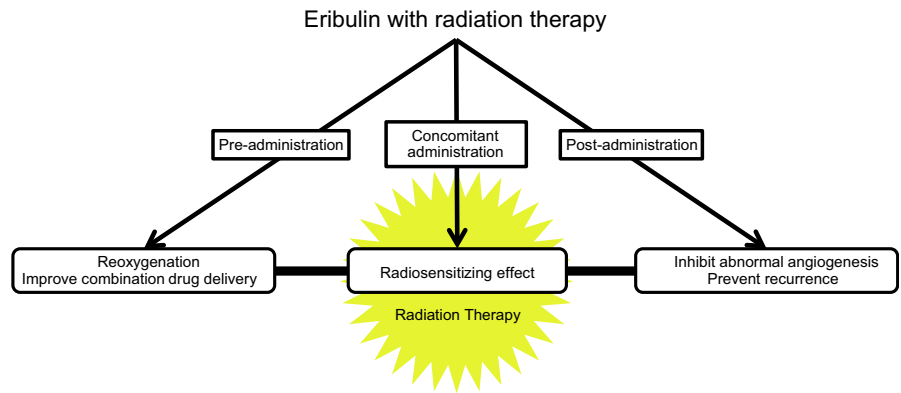
irradiation is beyond the scope of this study, it warrants further investigation.

Another mechanism for the effect of the combined eribulin and radiation treatment on synergistically suppressing tumor growth may be vascular remodeling conferred by eribulin. There have been several reports that demonstrate vascular normalization effects of eribulin on tumor microvasculature. In a preclinical human breast cancer model, Funahashi et al<sup>20</sup> showed that eribulin induced the remodeling of the vasculature in xenografted tumors and improved perfusion

in the tumor tissues, particularly in the tumor core. Ueda et al<sup>19</sup> examined breast cancer patients treated with eribulin using in vivo imaging and found that oxygen saturation in the tumor was significantly increased. Hypoxia is a well-known source of resistance to radiation and chemotherapy.<sup>36</sup> These findings suggest that eribulin may enhance the effect of radiation by re-oxygenating tumor tissues through vascular remodeling. In our study, a combination of eribulin and radiation treatment, whether eribulin was given before or after radiation, significantly reduced the mean vascular areas of



**FIGURE 5** Treatment strategy of eribulin administration combined with irradiation at 3 different phases: (i) pre-administration of eribulin reoxygenates the tumor core, increases the effect of radiation and increases drug delivery; (ii) concomitant administration of eribulin has a radiosensitizing effect; and (iii) maintenance administration of eribulin after radiation decreases the abnormal vascularization of irradiated tumors and may lead to sustained tumor control



xenografted brain tumor tissues compared with radiation treatment alone (Figure 4C). Treatment by eribulin alone also showed the tendency to reduce the mean vascular area in tumors as compared to untreated controls, although the difference did not reach statistical significance. Although our data are limited, these results support the notion that eribulin normalizes tumor microvasculature.

On the other hand, radiation itself also induces hypoxia.<sup>36-38</sup> Lesions in a tumor where abnormal blood vessels develop may be susceptible to hypoxia because of the unstable blood flow ("cycling hypoxia lesion"), possibly activating HIF-1.<sup>37</sup> Radiation could cause the lesion to become reoxygenated as a consequence of effective oxygenated tumor cell death. However, this may also generate reactive oxygen species (ROS) in the oxygenated lesion and stabilize HIF-1, eventually further enhancing angiogenesis to support tumor growth.<sup>36</sup> We showed that the combination of eribulin and radiation resulted in a significant decrease in MVA in xenografted mouse brain tumor tissues (Figure 4). A decrease in MVA has been associated with vascular remodeling in the tumor, which could lead to improved perfusion, oxygenation and drug delivery.<sup>19,20</sup> Thus, we consider that the vascular remodeling induced by eribulin may suppress radiation-induced angiogenesis and play a crucial role in the efficacy of the combined radiation and eribulin therapy by normalizing the microenvironment and inducing re-oxygenation. To confirm this hypothesis, further studies exploring hypoxic status in the tumor microenvironment are warranted.

It has also been reported that in breast cancer patients, bevacizumab non-responders showed higher degrees of angiogenesis with more severe hypoxia during bevacizumab treatment compared to responders.<sup>39</sup> Oxygen saturation in breast cancers was shown to increase in patients treated with eribulin but not in those treated with bevacizumab.<sup>19</sup> These data suggest that eribulin may also be beneficial to patients with GBM who do not respond to bevacizumab.

Another intriguing finding is that the continual administration of eribulin after concomitant treatment with eribulin and radiation resulted in a more sustained inhibition of tumor growth in intracerebral U87MG xenografts than eribulin alone (Figure 3B). It was particularly notable that only a single cycle (4 Gy  $\times$  3) of irradiation given in the first week, which did not improve the survival of the brain tumor-bearing mice on its own, was sufficient to significantly

enhance the life-prolonging effect of eribulin (Figure 2B). It is possible that the initial concomitant eribulin and radiation treatment was so effective at killing glioma cells that the maintenance administration of eribulin more efficiently controlled recurrence than eribulin alone. The mechanism of the prolonged cytostatic effect of maintenance eribulin when combined with radiation requires further investigation.

Taken together, we propose a new therapeutic strategy for GBM: a concomitant treatment with eribulin and radiation to radiosensitize tumor cells followed by a maintenance administration of eribulin. The concomitant treatment with eribulin radiosensitizes tumor cells to maximize the effect of radiation and rectify the hypoxia and abnormal angiogenesis induced by radiation. The maintenance eribulin treatment has an enhanced cytostatic effect on the remaining/surviving tumor cells (Figure 5). One limitation of our study is that we focused on the U87MG glioma cell line for the *in vivo* experiments, because it was a well-established brain tumor model. Biological behavior of gliomas is diverse, however, so it is possible that the response of other glioma cells to the concomitant eribulin and radiation treatment may be different. Nonetheless, we have previously confirmed that eribulin significantly prolonged survival of intracerebral xenografts of several patient-derived glioma cells (Takahashi, submitted). We therefore consider that the combined eribulin and radiation treatment would be effective in a wide range of gliomas. It is hoped that the new strategy will be effective even for GBM cases that are resistant to TMZ or bevacizumab. A clinical trial to test the efficacy of the combined treatment is warranted.

In summary, we showed that eribulin when combined with radiation efficiently suppressed the growth of engrafted mouse brain tumors, possibly through: (i) a radiosensitizing effect, possibly by either inducing M-phase arrest and/or an inhibitory effect on microtubule dynamics; (ii) the normalization of abnormal angiogenesis and reoxygenation of the microenvironment, which would lead to better radiosensitivity and local drug delivery; and (iii) a sustained cytostatic effect of the maintenance administration. Our ultimate aim is to establish a novel effective therapeutic strategy for newly diagnosed GBM. The concomitant eribulin and radiation treatment hopefully represents a step towards this goal.

**CONFLICT OF INTEREST**

Masamichi Takahashi received remuneration from Brainlab corporation. Yoshitaka Narita received honoraria from Chugai Pharmaceutical, and research funds from Abbvie, Ono Pharmaceutical, SBI Pharma, Stella-Pharma, Daiichi-Sankyo and Eisai. Ryo Nishikawa received honoraria and research funds from Eisai Koichi. Ichimura received a research grant from EPS Corporation, Chugai Pharmaceutical, Taiichi Sankyo and Eisai. The other authors have no conflicts of interest related to this work to declare.

**ORCID**

Koichi Ichimura  <http://orcid.org/0000-0002-3851-2349>

**REFERENCES**

- Stupp R, Mason WP, van den Bent MJ, et al. Radiotherapy plus concomitant and adjuvant temozolomide for glioblastoma. *N Engl J Med*. 2005;352:987-996.
- Cancer Genome Atlas Research N. Comprehensive genomic characterization defines human glioblastoma genes and core pathways. *Nature*. 2008;455:1061-1068.
- Parsons DW, Jones S, Zhang X, et al. An integrated genomic analysis of human glioblastoma multiforme. *Science*. 2008;321:1807-1812.
- Verhaak RG, Hoadley KA, Purdom E, et al. Integrated genomic analysis identifies clinically relevant subtypes of glioblastoma characterized by abnormalities in PDGFRA, IDH1, EGFR, and NF1. *Cancer Cell*. 2010;17:98-110.
- Osuka S, Van Meir EG. Overcoming therapeutic resistance in glioblastoma: the way forward. *J Clin Invest*. 2017;127:415-426.
- Lau D, Magill ST, Aghi MK. Molecularly targeted therapies for recurrent glioblastoma: current and future targets. *Neurosurg Focus*. 2014;37:E15.
- Bastien JI, McNeill KA, Fine HA. Molecular characterizations of glioblastoma, targeted therapy, and clinical results to date. *Cancer*. 2015;121:502-516.
- Cabrera AR, Kirkpatrick JP, Fiveash JB, et al. Radiation therapy for glioblastoma: executive summary of an American Society for Radiation Oncology Evidence-Based Clinical Practice Guideline. *Pract Radiat Oncol*. 2016;6:217-225.
- Pawlik TM, Keyomarsi K. Role of cell cycle in mediating sensitivity to radiotherapy. *Int J Radiat Oncol Biol Phys*. 2004;59:928-942.
- Oehler C, von Bueren AO, Furmanova P, et al. The microtubule stabilizer patupilone (epothilone B) is a potent radiosensitizer in medulloblastoma cells. *Neuro Oncol*. 2011;13:1000-1010.
- Mc Gee MM. Targeting the mitotic catastrophe signaling pathway in cancer. *Mediators Inflamm*. 2015;2015:146282.
- Gupta N, Hu LJ, Deen DF. Cytotoxicity and cell-cycle effects of paclitaxel when used as a single agent and in combination with ionizing radiation. *Int J Radiat Oncol Biol Phys*. 1997;37:885-895.
- An Z, Muthusami S, Yu JR, Park WY. T0070907, a PPAR gamma inhibitor, induced G2/M arrest enhances the effect of radiation in human cervical cancer cells through mitotic catastrophe. *Reprod Sci*. 2014;21:1352-1361.
- Towle MJ, Salvato KA, Budrow J, et al. In vitro and in vivo anticancer activities of synthetic macrocyclic ketone analogues of halichondrin B. *Cancer Res*. 2001;61:1013-1021.
- Okouneva T, Azarenko O, Wilson L, Littlefield BA, Jordan MA. Inhibition of centromere dynamics by eribulin (E7389) during mitotic metaphase. *Mol Cancer Ther*. 2008;7:2003-2011.
- Smith JA, Wilson L, Azarenko O, et al. Eribulin binds at microtubule ends to a single site on tubulin to suppress dynamic instability. *Biochemistry*. 2010;49:1331-1337.
- Towle MJ, Salvato KA, Wels BF, et al. Eribulin induces irreversible mitotic blockade: implications of cell-based pharmacodynamics for in vivo efficacy under intermittent dosing conditions. *Cancer Res*. 2011;71:496-505.
- Kuznetsov G, Towle MJ, Cheng H, et al. Induction of morphological and biochemical apoptosis following prolonged mitotic blockage by halichondrin B macrocyclic ketone analog E7389. *Cancer Res*. 2004;64:5760-5866.
- Ueda S, Saeki T, Takeuchi H, et al. In vivo imaging of eribulin-induced reoxygenation in advanced breast cancer patients: a comparison to bevacizumab. *Br J Cancer*. 2016;114:1212-1218.
- Funahashi Y, Okamoto K, Adachi Y, et al. Eribulin mesylate reduces tumor microenvironment abnormality by vascular remodeling in pre-clinical human breast cancer models. *Cancer Sci*. 2014;105:1334-1342.
- Taur JS, DesJardins CS, Schuck EL, Wong YN. Interactions between the chemotherapeutic agent eribulin mesylate (E7389) and P-glycoprotein in CF-1 abcb1a-deficient mice and Caco-2 cells. *Xenobiotica*. 2011;41:320-326.
- Sugawara M, Condon K, Liang E, et al. Eribulin shows high concentration and long retention in xenograft tumor tissues. *Cancer Chemother Pharmacol*. 2017;80:377-384.
- Chang AY, Ying XX. Brain metastases from breast cancer and response to treatment with eribulin: a case series. *Breast Cancer (Auckl)*. 2015;9:19-24.
- Matsuoka H, Tsurutani J, Tanizaki J, et al. Regression of brain metastases from breast cancer with eribulin: a case report. *BMC Res Notes*. 2013;6:541.
- Nieder C, Aandahl G, Dalhaug A. A case of brain metastases from breast cancer treated with whole-brain radiotherapy and eribulin mesylate. *Case Rep Oncol Med*. 2012;2012:537183.
- Byun KD, Ahn SG, Baik HJ, et al. Eribulin mesylate combined with local treatment for brain metastasis from breast cancer: two case reports. *J Breast Cancer*. 2016;19:214-217.
- Sunayama J, Sato A, Matsuda K, et al. Dual blocking of mTor and PI3K elicits a prodifferentiation effect on glioblastoma stem-like cells. *Neuro Oncol*. 2010;12:1205-1219.
- Sato A, Sunayama J, Okada M, et al. Glioma-initiating cell elimination by metformin activation of FOXO3 via AMPK. *Stem Cells Transl Med*. 2012;1:811-824.
- Tomiya A, Uekita T, Kamata R, et al. Flotillin-1 regulates oncogenic signaling in neuroblastoma cells by regulating ALK membrane association. *Cancer Res*. 2014;74:3790-3801.
- Hirai T, Shirai H, Fujimori H, Okayasu R, Sasai K, Masutani M. Radiosensitization effect of poly(ADP-ribose) polymerase inhibition in cells exposed to low and high linear energy transfer radiation. *Cancer Sci*. 2012;103:1045-1050.
- Schneider CA, Rasband WS, Eliceiri KW. NIH Image to ImageJ: 25 years of image analysis. *Nat Methods*. 2012;9:671-675.
- Takahashi M, Valdes G, Hiraoka K, et al. Radiosensitization of gliomas by intracellular generation of 5-fluorouracil potentiates prodrug activator gene therapy with a retroviral replicating vector. *Cancer Gene Ther*. 2014;21:405-410.
- Ovejera AA, Houchens DP, Barker AD. Chemotherapy of human tumor xenografts in genetically athymic mice. *Ann Clin Lab Sci*. 1978;8:50-56.
- McTye E, Scott J, Chinnaiyan P. Whole brain radiotherapy for brain metastasis. *Surg Neurol Int*. 2013;4:S236-S244.

35. Mendelsohn W. The significance of abnormal mitosis in the development of malignancy. *Am J Cancer*. 1935;24:626-636.
36. Dewhirst MW, Cao Y, Moeller B. Cycling hypoxia and free radicals regulate angiogenesis and radiotherapy response. *Nat Rev Cancer*. 2008;8:425-437.
37. Barker HE, Paget JT, Khan AA, Harrington KJ. The tumour microenvironment after radiotherapy: mechanisms of resistance and recurrence. *Nat Rev Cancer*. 2015;15:409-425.
38. Dewhirst MW. Relationships between cycling hypoxia, HIF-1, angiogenesis and oxidative stress. *Radiat Res*. 2009;172:653-665.
39. Ueda S, Saeki T, Osaki A, Yamane T, Kuji I. Bevacizumab induces acute hypoxia and cancer progression in patients with refractory breast cancer: multimodal functional imaging and multiplex cytokine analysis. *Clin Cancer Res*. 2017;23:5769-5778.

#### SUPPORTING INFORMATION

Additional supporting information may be found online in the Supporting Information section at the end of the article.

**How to cite this article:** Miki S, Imamichi S, Fujimori H, et al. Concomitant administration of radiation with eribulin improves the survival of mice harboring intracerebral glioblastoma. *Cancer Sci*. 2018;109:2275-2285.  
<https://doi.org/10.1111/cas.13637>